Colored-noise-induced Hopf bifurcations in predator-prey communities

Romi Mankin, Tõnu Laas,* Ako Sauga, and Ain Ainsaar
Department of Natural Sciences, Tallinn University, 25 Narva Road, 10120 Tallinn, Estonia

Eerik Reiter
Institute of Physics, Tallinn University of Technology, 5 Ehitajate Tee, 19086 Tallinn, Estonia
(Received 21 February 2006; published 1 August 2006)

A broad class of $(N+1)$-species ratio-dependent predator-prey stochastic models, which consist of one predator population and N prey populations, is considered. The effect of a fluctuating environment on the carrying capacities of prey populations is taken into account as colored noise. In the framework of the mean-field theory, approximate self-consistency equations for prey-populations mean density and for predator-population density are derived (to the first order in the noise variance). In some cases, the mean field exhibits Hopf bifurcations as a function of noise correlation time. The corresponding transitions are found to be reentrant, e.g., the periodic orbit appears above a critical value of the noise correlation time, but disappears again at a higher value of the noise correlation time. The nonmonotonous dependence of the critical control parameter on the noise correlation time is found, and the conditions for the occurrence of Hopf bifurcations are presented. Our results provide a possible scenario for environmental-fluctuations-induced transitions between the oscillatory regime and equilibrium state of population sizes observed in nature.

DOI: 10.1103/PhysRevE.74.021101 PACS number(s): 05.40.−a, 87.10.+e

I. INTRODUCTION

Many physical, chemical, and biological processes can be considered as general nonlinear systems in which oscillatory motion is influenced by external noise [1–3]. At that, the phenomenon of coherence resonance is of great importance. Remarkably, even in the absence of external periodic influence noise can induce regular and, at a certain noise level, maximally coherent oscillations of state variables [4,5]. Experimentally, the phenomenon of coherence resonance close to the onset of a Hopf bifurcation has been observed for plasma waves [6], electrochemical reactions [7], and a semiconductor laser with short optical feedback [1].

One of the key issues in ecology is how environmental fluctuations and species interactions determine the oscillations in population sizes displayed by many organisms in nature as well as in laboratory cultures [8–10]. Ecologists have mainly been interested in the dynamical consequences of population interactions, often ignoring environmental variability altogether. However, the essential role of environmental fluctuations has recently been recognized in theoretical ecology. Noise-induced effects on population dynamics have been subject to intense theoretical investigations [11,12]. Moreover, ecological investigations suggest that population dynamics is sensitive to noise color [13]. In spite of the obvious significance of this circumstance, the role of nonequilibrium fluctuations (colored noise) of environmental parameters has not been investigated much in the context of ecosystems [12].

After the seminal models of Volterra and Lotka, the dynamical relationship between prey and their predators has been studied extensively in ecology due to its universal existence and importance [14]. The general deterministic (without fluctuations) model for predator-prey dynamics, in its classical form, can be written as [10,15]

$$\frac{dx}{dt} = f(x)x - \alpha g(x,y)y,$$

$$\frac{dy}{dt} = \beta g(x,y)y - dy, \tag{1}$$

where x and y are densities of prey abundance and predator abundance, respectively, $f(x)$ is per capita rate of increase of the prey in the absence of predation, and d is food-independent predator mortality, assumed to be constant. The function αg describes the amount of prey consumed per predator per unit time, while βg describes predator production per capita. The quotient of two constants β and α is the conversion efficiency β/α. The most popular models [16] that have been used to interpret the behavior of many predator-prey communities assume that the predator functional response $g(x,y)$ is determined by prey abundance x as the only variable: $g=g(x)$ (the so-called prey-dependent model). However, the model accounts for the relationships between prey and predator populations in case individuals are uniformly distributed in space and their age structure and sex ratio do not significantly affect the growth rate of either population. Recently, there is growing biological and physiological evidence that in many situations, especially in complex, heterogeneous systems, where the large-scale outcome of predation is a sharing process (the predators have to search or compete for food), a more adequate predator-prey theory should be based on a ratio-dependent model [17]. Generally, the ratio-dependent model states that the per capita predator growth rate should be a function of the ratio of prey to predator abundance, i.e., the predator functional response $g=g(x/y)$. This statement is strongly supported by numerous field and laboratory experiments and observations

*Electronic address: tony@tlu.ee

[18]. Mathematical analysis shows that ratio-dependent models are capable of producing richer and biologically more reasonable or acceptable dynamics than the traditional prey-dependent models [15,19,20].

Although deterministic ratio-dependent predator-prey models are useful in modeling many real ecological communities, there is almost nothing available either on qualitative analysis of multispecies interaction or on the effect of environmental fluctuations in models based on a ratio-dependent approach. It is of interest, both from theoretical and practical viewpoints, to know whether the transitions from equilibrium states to oscillatory regimes (and the opposite way) sometimes occurring in ecosystems [8–10] could be regarded as induced by environmental nonequilibrium fluctuations.

Thus motivated, we have written this paper, considering a broad class of $(N+1)$-species ratio-dependent predator-prey models that consist of one predator population and N prey populations. The effect of a fluctuating environment on the growth of prey populations is modeled as nonequilibrium fluctuations of the carrying capacities (multiplicative colored noise).

Since one of the characteristic quantities of an ecosystem, perhaps the most fundamental one, is its average species density [21] ($\Sigma_{i=1}^{N} X_i/N$, where X_i is the population density of the ith species), we consider the average species density of preys as one of the two state parameters of an ecosystem, the other state parameter being the density of predator abundance. We study the model using a mean-field approach, focusing on colored-noise-induced Hopf bifurcations. For the sake of mathematical simplicity, we confine ourselves to the case where the noise is a symmetric zero-mean exponentially correlated Markovian stochastic process with a sufficiently small dispersion.

The main contribution of this paper is as follows. We establish two types of colored-noise-induced Hopf bifurcations and give the necessary and sufficient conditions for the appearance of such effects. Namely, depending on the mutual interplay of the prey's self-regulation mechanism and predator dynamics, an increase of noise correlation time can induce transitions from an equilibrium state to the stable limit cycle (with some oscillations of population abundance) as well as in the opposite direction. Furthermore, both transition types are found to be reentrant, e.g., the limit cycle appears above a critical value of the noise correlation time, but disappears again through reentrant transition to the equilibrium state at a higher value of the noise correlation time. To our knowledge, the appearance of colored-noise-induced Hopf bifurcations and corresponding reentrant transitions in models of ecosystems have not been described before.

We also analyze the role of the parameters of the generalized Verhulst self-regulation mechanism (GVM) in such transitions. It is shown that the ratio-dependent models with the GVM for the prey populations

$$f_i(X_i) = \delta\left[1 - \left(\frac{X_i}{K_i}\right)^c\right], \tag{2}$$

where δ and c are constants, $X_i (i=1,\ldots,N)$ is the population density of the ith species, and K_i is the carrying capacity, are more sensitive to environmental fluctuations if the exponent c is greater. This means that the growth of the exponent c will increase that region of the phase space of the system parameters, where Hopf bifurcations in noise correlation time are possible.

The structure of the paper is as follows. Section II presents a brief review of the properties of the deterministic ratio-dependent model (1). The basic model investigated in this work is presented, and a mean-field description of the model is given. The corresponding self-consistency equation is found. In Sec. III, the behavior of the self-consistently determined prey and predator densities is analyzed. The phenomenon of Hopf bifurcations in noise correlation time is established, and the dependence of the critical capturing rate α_{cr} on the noise correlation time and other system parameters is investigated. Section IV contains some brief concluding remarks. Some calculations and formulas are relegated to the Appendix.

II. MODEL

A. Deterministic ratio-dependent predator-prey system

Recently, a complete mathematical description of the Michaelis-Menten-type ratio-dependent predator-prey system (1) with

$$f(x) = \left(1 - \frac{x}{K}\right), \quad g\left(\frac{x}{y}\right) = \frac{x}{x+y},$$

where K is the carrying capacity of the prey, have been the topic of a number of investigations [15,19,20]. The main objective of those papers is to consider the stability behavior of solutions around different equilibrium points (x_e, y_e) with special emphasis on the controversial equilibrium point (0, 0) in the ratio-dependent model. The controversy about the equilibrium point (0, 0) is due to the fact that ratio-dependent models are undefined at (0, 0), e.g., the model system cannot be linearized at (0, 0). The authors of Ref. [15] have proved for a general ratio-dependent model that the point (0, 0) can become attractive for all initial conditions sufficiently close to the predator axis, while the nontrivial equilibrium remains either locally stable or becomes unstable. This gives rise to global behaviors that range from global attractivity of the nontrivial equilibrium, and coexistence of two different attractors to global attractivity of the equilibrium (0, 0) [15].

The Michaelis-Menten-type ratio-dependent system (1) described above has two equilibria, $E_1=(0,0)$ and $E_2=(K,0)$ on the x axis for all possible values of the parameters α, β, and d. The third equilibrium point $E_3=(x_s,y_s)$, i.e., the nontrivial equilibrium is given by

$$x_s = K[1-\alpha(1-r)], \quad y_s = \frac{(1-r)}{r}x_s, \quad r := \frac{d}{r}.$$

This equilibrium is biologically meaningful $(x_s>0, y_s>0)$ only if $\alpha<1/(1-r)$, $0<r<1$.

The stability analysis of E_3 shows that the equilibrium $(x_s>0, y_s>0)$ is locally stable if $\alpha<\bar{\alpha}\equiv\min\{1/(1-r), [1+d(1-r)]/(1-r^2)\}$. In the case of $d<\beta<1+d$ and

$\alpha=\alpha_{cr}\equiv[1+d(1-r)]/(1-r^2)$, the system exhibits a Hopf-bifurcation near E_3. It is shown that the corresponding Hopf-bifurcation is supercritical [19,20].

Relying on [19], we briefly review some global properties of the model. By the change of variables $(x,y)\rightarrow(u,y)$, where $u=x/y$, the system can be transformed into a Gause-type predator-prey system where an analysis of solutions around the origin (0, 0) is feasible. The transformed system in the case of $d<\beta<1+d$, $1+d<\alpha<1/(1-r)$ has three equilibria: $E_1^*=(0,0)$, $E_2^*=(\Theta_0,0)$, and $E_3^*=(u_s,y_s)$. The equilibrium E_1^* is locally asymptotically stable, E_2^* is a saddle point, and E_3^* is unstable if $\Theta_0<u_s<\Theta_1=\Theta_0+\sqrt{\Theta_0(\Theta_0+1)}$ and stable if $u_s>\Theta_1$, where $\Theta_0=[\alpha-(1+d)]/[(1+d)-\beta]$. Note, that Θ_0 and Θ_1 are positive zeros of $h(u)$ and $h'(u)$, respectively. The function $h(u)$ is determined by the prey isocline

$$y=h(u)\equiv K[1+d-\alpha+u(1+d-\beta)]\frac{1}{u(u+1)}.$$

The behavior of the stable manifold Γ of E_2^* can be classified as follows: (i) if Γ intersects the prey isocline, then Γ connects E_2^* and E_3^*; (ii) if Γ does not intersect the prey isocline $y=h(u)$, then $\Gamma'=\Gamma^*$ of Γ' lies above Γ^* where $\Gamma'=\{(x,y):x=y\cdot u,(u,y)\in\Gamma\}$ and Γ^* is an unstable manifold of the equilibrium $E_2=(K,0)$, connecting $(K,0)$ to (0, 0) or (x_s,y_s) in (x,y)-plane.

It is shown that in case the ratio at equlibrium (x_s/y_s) is large, i.e., $x_s/y_s=r/(1-r)\geqslant\Theta_1$, and if $x(0)/y(0)$ is small, then both predators and preys go to extinction, whereas if $x(0)/y(0)$ is large, then predators and preys coexist in the form of equilibrium E_3. In the case of $\Theta_0<x_s/y_s<\Theta_1$, there are three alternatives: (i) There is an orbit Γ' connecting E_1 and E_3. In this case, except if $[x(0),y(0)]\in\Gamma'$, both predators and preys go to extinction. (ii) The unstable manifold Γ^* of the equilibrium $E_2=(K,0)$ is connected to the origin (0, 0). For $[x(0),y(0)]$ above Γ^*, both predators and preys go to extinction, while for $[x(0),y(0)]$ below Γ^*, $[x(0),y(0)]\neq(x_s,y_s)$, the predator and prey populations oscillate aperiodically (a heteroclinic cycle is the global attractor). (iii) This case is similar to case (ii). The only difference is that for $[x(0),y(0)]$ below Γ^*, the solution approaches a unique stable limit cycle. Thus, both the predator and prey populations exhibit periodic oscillations. (e.g., the occurrence of the Hopf-bifurcation). Finally, we emphasize that the dynamical behavior of the deterministic ratio-dependent predator-prey model (1) with logistic self-regulation is independent of the carrying capacity of the prey.

B. Stochastic model

As was mentioned in the introduction, the present model is based on the generalization of the ratio-dependent model for predator-prey dynamics (1) to the case of one predator population and N prey populations:

$$\frac{dX_i}{d\tilde{t}}=f_i(X_i)X_i-\tilde{\alpha}g\left(\frac{\bar{x}}{y}\right)\frac{y}{\bar{x}}X_i,$$

$$\frac{dy}{d\tilde{t}}=\tilde{\beta}g\left(\frac{\bar{x}}{y}\right)y-\tilde{d}y, \tag{3}$$

where $X_i(\tilde{t})$ $(i=1,\ldots,N)$ is the density of the ith prey population at the time $\tilde{t}$, $y(\tilde{t})$ is the density of the predator population, and $\bar{x}(\tilde{t})=(1/N)\Sigma_{i=1}^{N}X_i(\tilde{t})$ is the average of the prey-population densities. The positive constants $\tilde{\alpha}$, $\tilde{\beta}$, and $\tilde{d}$ stand for the prey capturing rate, maximal predator growth rate, and predator death rate, respectively. Here we have assumed that for consumers (predator), all prey populations are equivalent, so that the function $\tilde{\alpha}g(\bar{x}/y)\cdot X_i/\bar{x}$ describes the amount of the ith prey consumed per predator per unit time. Model (3) is biologically meaningful only if the functional response g is bounded, non-negative and increasing, and equal to zero at zero:

$$0\leqslant g\left(\frac{\bar{x}}{y}\right)<1,\quad 0\leqslant\frac{\bar{x}}{y}<\infty. \tag{4}$$

Here we remember that $\tilde{\beta}$ is the maximal predator growth rate. The function $f_i(X_i)$ describes the development of the ith species without any interaction with other species. A typical mechanism for self-regulation in ecosystems includes, for example, a territorial breeding requirement and the crowding effect caused by competition for resources [21]. These are taken into account by applying the generalized Verhulst model (2) with $c>0$.

Environmental fluctuations are important components in an ecosystem. In Ref. [16], May pointed out the fact that because of environmental fluctuations, the carrying capacities, death rates, birth rates, and other parameters involved with the model system exhibit random fluctuations to a greater or lesser extent. Because a multinoise stochastic system is difficult to consider analytically, it is reasonable, for the sake of mathematical simplicity, to confine to the case where but one of system parameters fluctuates (at least at the initial stage of investigations). As in the deterministic counterpart of model (3), the appearance of Hopf bifurcations is independent of the carrying capacity K but depends on other system parameters (cf. Sec. II A), it is of interest to know, whether colored fluctuations of the carrying capacities can induce Hopf bifurcations in the system (3).

Thus motivated, a random interaction with the environment (climate, diseases, etc.) is taken into account by introducing a colored noise in $f_i(X_i)$. From now on we shall use fluctuations of the carrying capacity

$$K_i=K[1+aZ_i(\tilde{t})], \tag{5}$$

where the colored noise $aZ_i(\tilde{t})$ is assumed to be a symmetric zero-mean exponentially correlated Markovian stochastic process with a being constant and

$$\langle aZ_i(\tilde{t})\rangle=0,\quad \langle aZ_i(\tilde{t}),aZ_j(\tilde{t}')\rangle=\delta_{ij}a^2\exp(-\tilde{\nu}|\tilde{t}-\tilde{t}'|). \tag{6}$$

Obviously, the noise correlation time $\tilde{\tau}_c=1/\tilde{\nu}$. The variance (a^2) of the noise is given by the square of its amplitude a.

Note that if noise is absent and the distribution of the initial prey-population abundances is uniform, $x_i(0)=x_0$, then model (3) reduces to the deterministic ratio-dependent model (1) for $\bar{x}$ and y. Thus, in this case, the results described in Sec. II. A are immediately applicable.

It is practicable, by applying a scaling of the form

$$t=\delta\tilde{t}, \quad \nu=\frac{\tilde{\nu}}{\delta}, \quad \alpha=\frac{\tilde{\alpha}}{\delta}, \quad \beta=\frac{\tilde{\beta}}{\delta}, \quad d=\frac{\tilde{d}}{\delta}, \tag{7}$$

to get a formulation of the dynamics with a dimensionless time t.

To proceed further with the analytical examination of model (3) with GVM, we follow the mean-field approximation scheme. We assume that $N\to\infty$. This means that we are interested in the case of a very great number of prey populations (or subpopulations in a prey metapopulation). The mean-field approximation can be reached by replacing the size average $\bar{x}=(1/N)\Sigma_{i=1}^{N}X_i(t)$ by the statistical average $\langle X(t)\rangle$ in Eqs. (3). In the case of a sufficiently small noise dispersion, $a^2\ll 1$, after quite simple calculations one can find the self-consistency equations for the Weiss mean-field approach, whose solution yields the dependence of $\langle X(t)\rangle$ and $y(t)$ on the system parameters (see the Appendix). The corresponding self-consistency equations are

$$\left[\frac{d}{dt}+\nu+c\gamma x^c-(c+1)\frac{\dot{x}}{x}\right]\left[\frac{d}{dt}+2\gamma c x^c-(c+1)\frac{\dot{x}}{x}\right]\times\left[\dot{x}-x+\gamma x^{c+1}+\alpha y g\left(\frac{x}{y}\right)\right]-c^3\gamma^2(1+c)a^2x^{2c}[\dot{x}+\gamma x^{c+1}]=0,$$

$$\frac{dy}{dt}=y\left[\beta g\left(\frac{x}{y}\right)-d\right], \tag{8}$$

where $x\equiv\langle X(t)\rangle$, $\gamma=K^{-c}[1+(c/2)(1+c)a^2]$, and $\dot{x}\equiv dx/dt$. First, it seems that the variance of noise a^2 and the switching rate of noise ν enter in Eqs. (8), independently. The "paradoxiality" of this circumstance disappear as we consider Eqs. (8) with initial conditions (A4). The first differential equation in Eqs. (8) with initial conditions (A4) is equivalent to the integral equation (A3), where in the absence of noise, $a^2=0$, the third-order differential equation in Eqs. (8) reduces to the second-order differential equation

$$\left[\frac{d}{dt}+2\gamma c x^c-(c+1)\frac{\dot{x}}{x}\right]\left[\dot{x}-x+\gamma x^{c+1}+\alpha y g\left(\frac{x}{y}\right)\right]=0,$$

which is independent of the switching rate ν.

Clearly, all the biologically meaningful solutions and initial conditions for $x(0)$ and $y(0)$ must lie within the positive quadrant $\{(x,y): x\geqslant 0, y\geqslant 0\}$. The system (8) has at most three kinds of equilibria in the positive quadrant: (i) trivial equilibrium $E_1(0,0)$—extinction of the ecosystem; (ii) axial equilibrium $E_2(x_s^*,0)$ with $x_s^*=K\{1-\nu a^2(c+1)/[2(c+\nu)]\}+O(a^4)$—extinction of the predator population; (iii) a nontrivial equilibrium (positive interior equilibrium) $E_3(x_s,y_s)$ with

$$y_s=x_sG(r), \quad r:=\frac{d}{\beta},$$

$$x_s=K[1-\alpha rG(r)]^{1/c}\left\{1-\frac{\nu a^2(c+1)}{2[\nu+c-\alpha crG(r)]}\right\}+O(a^4), \tag{9}$$

where $G(r):=1/[g^{-1}(r)]$ and g^{-1} is the inverse function of g. Note that the nontrivial equilibrium E_3 is possible if

$$d<\beta, \quad \alpha<\bar{\alpha}:=\frac{1}{[rG(r)]}, \tag{10}$$

i.e., the predators and preys coexist in equilibrium provided the maximal predator growth rate is larger than its death rate and the prey capturing rate α is sufficiently small.

In Sec. III, we confine ourselves to case (10) and mainly consider the local stability of the system around the equilibrium $E_3(x_s,y_s)$, which is one of the most interesting equilibrium from the biological point of view. Although the behavior of the system near the extinction is not less biologically interesting (cf. Sec. II A), we relegate corresponding analysis to future investigations. Particularly, the singular behavior of Eqs. (8) at $x=0$ set up a necessity for another mathematical technique, e.g., a description in the spirit of Ref. [19] (see also the comments in Sec. II A).

III. RESULTS

Our next task is to find the stability condition of the nontrivial equilibrium $E_3(x_s,y_s)$. The study of the stability plays a significant role in understanding the structure and functions of ecological systems [9,16,20]. An equilibrium point is called a stable equilibrium if perturbed populations will return to the equilibrium point in the course of time. The return may be either in the form of damped oscillations or monotonic.

Equations (8) become a four-dimensional dynamical system of x, $\dot{x}$, $\ddot{x}$, and y. A standard linear stability analysis [22] evaluated at $(x_s,0,0,y_s)$ yields the characteristic equation for the eigenvalues λ of the Jacobian matrix

$$\left\{(\lambda+2c\gamma x_s^c)(\lambda+\nu+c\gamma x_s^c)-\frac{\nu a^2c^3(c+1)[1-\alpha rG(r)]^2}{\nu+c[1-\alpha rG(r)]}\right\}\times\left\{\lambda^2+\lambda\left[\omega+c-\alpha rG(r)\left(1+c-\frac{\omega}{d}\right)\right]+\omega c[1-\alpha rG(r)]\right\}+\lambda\alpha rG(r)\times\frac{\nu a^2c^3(c+1)[1-\alpha rG(r)]^2}{\nu+c[1-\alpha rG(r)]}\left(\frac{\omega}{d}-1\right)=O(a^4), \tag{11}$$

where

$$\omega:=\beta\left[\xi\frac{d}{d\xi}g(\xi)\right]_{|\xi=1/G(r)}. \tag{12}$$

To find a condition for the capturing rate α corresponding to the Hopf bifurcation of $(x_s,0,0,y_s)$, we substitute $\lambda=i\Omega$

in Eq. (11). This shows that the characteristic polynomial has a pair of purely imaginary roots $\lambda_{1,2}=\pm i\Omega$, $\Omega>0$, if

$$\alpha=\alpha_{cr}=\frac{\beta}{G(r)}\frac{(\omega+c)}{[(1+c)d-\omega]}\times\left\{1-\frac{\nu a^2 c(c+1)\eta^2(\omega+\eta)[2(\nu+\eta)-\omega]}{(\nu+\eta)(\omega+c)(4\eta+\omega)[(\nu+\eta)^2+\eta\omega]}\right\}+O(a^4), \tag{13}$$

with

$$\eta:=\frac{c[d-(1+d)\omega]}{[(1+c)d-\omega]}. \tag{14}$$

It is easy to check that the equilibrium point is stable if $\alpha<\alpha_{cr}$, and unstable if $\alpha>\alpha_{cr}$.

The transition is caused by a simple pair of complex-conjugate eigenvalues crossing the imaginary axis at $\lambda=\pm i\Omega$, where

$$\Omega^2=\omega\eta+O(a^2). \tag{15}$$

The velocity of the crossing is nonzero, and the third and fourth eigenvalues, $\lambda_3\approx-2c\gamma x_s^c$, $\lambda_4\approx-(\nu+c\gamma x_s^c)$, remain negative for nearby parameter values. Thus, a Hopf bifurcation takes place at $\alpha=\alpha_{cr}$ [22]. Moreover, our numerical calculations based on Eqs. (8) and (A4) clearly show [particularly in the case of the Michaelis-Menten-type ratio-dependent functional response, $g(x/y)=x/(x+y)$] that the corresponding Hopf-bifurcations are supercritical (cf. also Fig. 1). From the imaginary part of the eigenvalues $\lambda_{1,2}$ the period of oscillation near the bifurcation point is approximately given by

$$T\approx\frac{2\pi}{\sqrt{\omega\eta}}. \tag{16}$$

It can be seen that the oscillation period T decreases monotonically as the exponent c in the generalized Verhulst self-regulation mechanism increases. We have noted earlier that the conditions (10) are necessary for the existence of the equilibrium point (x_s,y_s). Hence, the necessary conditions for the appearance of Hopf bifurcations are

$$d<\beta,\quad \omega<\frac{d}{1+d}, \tag{17}$$

i.e., $\bar{\alpha}>\alpha_{cr}$. Note, that at $\omega=d/(1+d)$ the parameter η in Eq. (14) vanishes and at $\alpha=\alpha_{cr}$ the equilibrium (x_s,y_s) tends to the point (0, 0), i.e., the limit cycle is not possible and the predator-prey system goes to extinction.

The above result establishes the existence of a small-amplitude periodic solution near the interior equilibrium point (x_s,y_s). The formula (13) for the critical capturing rate α_{cr} is the most important result of this work. Notably, Eq. (13) demonstrates that the functional dependence of α_{cr} on the noise correlation time $\tau_c=1/\nu$ exhibits a resonance form as τ_c is varied.

The typical forms of the graph of $\alpha_{cr}(\nu)$ are represented in Fig. 2. At the conditions of (17), one has to discern two cases. First, if $\omega<2\eta$, then the function $\alpha_{cr}(\nu)$ has a minimum α_{cr1} at a certain finite value ν_m of the noise-switching rate ν. At a long-correlation-time limit, $\nu\to0$, and also in the fast-noise limit, $\nu\to\infty$, the critical capturing rate α_{cr} saturates at the value

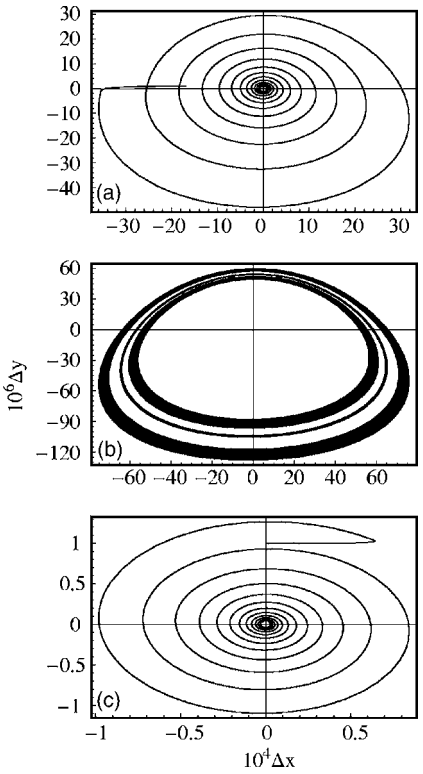

FIG. 1. The emergence of the Hopf bifurcation (and reentrant transition) to noise correlation time variations $[\Delta y:=y(t)-y_s, \Delta x:=x(t)-x_s]$. The orbits are computed by means of Eqs. (8), (19), and (A4), at the parameter values $c=b=\gamma=1$, $\beta=0.00078$, $d=0.0005$, $\alpha=1.696216$, $a^2=0.01$, and $\sigma^2=\chi=0$. (a) Stable focus at the noise switching rate $\nu=0.01$. Note that $\alpha<\alpha_{cr}(\nu)=1.697688$. (b) The stable limit cycle (the closed middle curve in the figure) at a moderate value of the switching rate $\nu=0.5$, $\alpha_{cr}(\nu)<\alpha<\alpha_{cr0}$. (c) The stable equlibrium point and orbit computed at the switching rate $\nu=10$. The initial conditions are: $x_0=0.391250$ and $y_0=0.219101$. The corresponding equilibrium point is determined by $x_s=0.391249$ and $y_s=0.219000$, while the condition $\alpha<\alpha_{cr}(\nu)=1.697609$ is fulfilled. For more details of panels (a), (b), and (c) see the text.

$$\alpha_{cr0}=\frac{\beta(\omega+c)}{G(r)[(1+c)d-\omega]}, \tag{18}$$

which corresponds to the critical capturing rate at absence of noise. Second, in the case of $\omega>2\eta$, there are always two extrema of $\alpha_{cr}(\nu)$. For increasing values of ν, the critical capturing rate starts from the value determined by Eq. (18), increasing to a local maximum α_{cr2}, next it decreases, attaining a local minimum α_{cr3}, and then α_{cr} approaches α_{cr0} as $\nu\to\infty$ [see Fig. 2(b)]. Since the appearance of a Hopf bifurcation in model (3) is independent of the carrying capacity K [see Eqs. (10), (13), and (17)], the asymptotic behavior of $\alpha_{cr}(\nu)$ has a distinct physical meaning. In the case of the adiabatic limit, $\nu\to0$, transitions between states of nonequi-

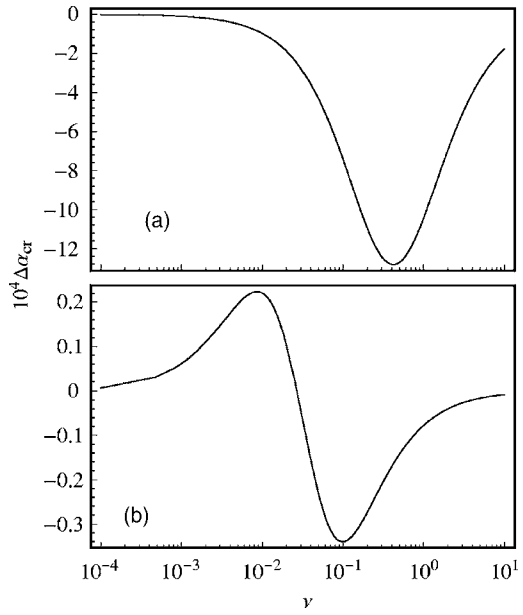

FIG. 2. The dependence of the critical capturing rate α_{cr}, $\Delta\alpha_{cr} := \alpha_{cr} - \alpha_{cr0}$, on the noise switching rate ν, obtained from Eqs. (13) and (14). The noise variance $a^2=0.01$, the parameter $c=1$, and α_{cr0} is computed from Eq. (18). (a) The case of $\omega<2\eta$: $d=0.5$, $\beta=0.78$, $\omega=0.179487$, and $G(r)=0.56$. The critical capturing rate by absence of noise $\alpha_{cr0}=2.002230$. (b) The case of $\omega>2\eta$: $d=0.1$, $\beta=0.92$, $\omega=0.0891$, $G(r)=8.2$, and $\alpha_{cr0}=1.102150$. Note the nonmonotonous dependence of α_{cr} on ν.

librium noise $Z(t)$ are so rare that the system has enough time to allow a deterministic dynamic to be formed between the transitions. At the fast-noise limit, i.e., at very high frequencies of colored fluctuations, the system is under the influence of the average

$$K_{\text{eff}}^{-c} := \langle K_i^{-c} \rangle \approx K^{-c}\left(1 + \frac{a^2(c+1)c}{2}\right).$$

Hence, the influence of fast fluctuations on an ecosystem can be biologically interpreted as a reduction of the carrying capacity K of a single species in Eqs. (2) and (3). The reduced (effective) carrying capacity K_{eff} reads: $K_{\text{eff}} \approx K[1-(a^2/2)\times(c+1)]$. Thus, our model with noise is, in the case of $\nu\to\infty$, equivalent to a deterministic model with the carrying capacity K_{eff}. Though we are not aware of any simple physical explanation for the nonmonotonous behavior of $\alpha_{cr}(\nu)$ at intermediate values of the correlation time, this behavior is not surprising if we remember that there is a phenomenon of autonomous stochastic parametric resonance, which generates an increase of the amplitude of oscillations [23].

The phenomenon of nonmonotonic behavior in noise correlation time of self-sustained oscillations under an influence of multiplicative colored noise in some nonlinear models has been studied in the context of coherence resonance [24]. Moreover, in those models, in contrast to ours, stochastic versions of the dynamics are obtained by substituting the deterministic control parameter of bifurcations by a noise-dependent parameter. Hence, the mechanism of noise-induced effects in the model considered here and in the models of Ref. [24] are of qualitatively different nature.

Relying on Fig. 2 and Eq. (13), one can find the necessary and sufficient conditions for the emergence of the Hopf bifurcation (and reentrant transition) due to noise correlation time variations. (i) The case of $\omega<2\eta$, $\alpha_{cr1}<\alpha<\alpha_{cr0}$ is characterized by the following scenario: For small values of the switching rate, $\nu<\nu_1$, where $\alpha<\alpha_{cr}(\nu)$, the system is in a stable equilibrium state (x_s,y_s). At $\nu=\nu_1$, i.e., $\alpha=\alpha_{cr}(\nu_1)$, the equilibrium point (x_s,y_s) becomes locally unstable and the system exhibits a Hopf bifurcation near (x_s,y_s). In the interval $\nu_1<\nu<\nu_2$ of the switching rate, there exists a limit cycle around (x_s,y_s), where both the predator-population and average prey-population densities oscillate. At $\nu=\nu_2$, where $\alpha=\alpha_{cr}(\nu_2)$, the limit cycle disappears and the system approaches a new stable equilibrium state (x_s,y_s), thus making a reentrant transition. The further increase of $\nu>\nu_2$ causes just a monotonic decrease of the equilibrium state parameters x_s and y_s [cf. Eq. (9)]. (ii) In the case of $\omega>2\eta$, there are two possible regimes of noise-induced transitions, depending on the value of the capturing rate α. First, if $\alpha_{cr0}<\alpha<\alpha_{cr2}$, where α_{cr2} is the maximal value of α_{cr}, for small values of $\nu<\nu_1^*$, $\alpha=\alpha_{cr}(\nu_1^*)$, the system evolves to a limit cycle. At $\nu=\nu_1^*$ the limit cycle disappears and the system evolves to a stable equilibrium point (x_s,y_s). Now, at $\nu=\nu_2^*>\nu_1^*$, $\alpha=\alpha_{cr}(\nu_2^*)$, the Hopf bifurcation appears (reentrant transition) and further on the system behaves according to a stable limit cycle. Second, if $\alpha_{cr3}<\alpha<\alpha_{cr0}$ (α_{cr3} is the minimal value of α_{cr}), then the behavior of the system is qualitatively the same as described in case (i), [cf. also Figs. 2(a) and 2(b)]. In Fig. 1 the scenario (i) described above is illustrated in the case of logistic self-regulation, $c=1$, and of the following Michaelis-Menden-Holling–type predator functional response

$$g\left(\frac{x}{y}\right) = \frac{x}{x+by}, \tag{19}$$

where $b>0$ is a constant. Note that in this case

$$G(r) = \frac{1-r}{br}, \quad \omega = d(1-r), \quad r \equiv \frac{d}{\beta}. \tag{20}$$

All orbits in Fig. 1 are computed from Eq. (8).

In Fig. 1(a), we plot an orbit in the state space (x,y) starting at $x_0=0.391250$, $y_0=0.219101$. The initial derivatives $\dot{x}(0)$ and $\ddot{x}(0)$ are given by Eqs. (A4). The parameters are such that $\alpha<\alpha_{cr}(\nu)$, $\omega<2\eta$, and the noise switching rate is small $\nu=0.01$. The spiral form of the orbit demonstrates that the equilibrium point $x_s=0.391249$, $y_s=0.219100$ is a stable focus. The "unusual" behavior of the orbit near the initial point (x_0,y_0) is caused by the circumstance that the dynamics of the system evolves in the four-dimensional space $(x,\dot{x},\ddot{x},y)$, where the orbit fast tends to a two-dimensional attracting center manifold. Figure 1(c) exhibits an analogous situation in the case of a "large" value of the switching rate $\nu=10$, i.e., after the reentrant transition.

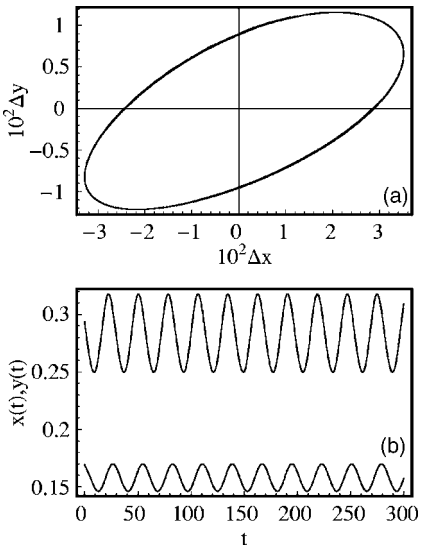

FIG. 3. (a) Stable limit cycle around the equilibrium point, $\Delta x=x(t)-x_s$, $\Delta y=y(t)-y_s$, $x_s=0.282641$, $y_s=0.158279$, for the system (8) with Eqs. (19) and (A4) at $a^2=0.01$, $d=0.5$, $\beta=0.78$, $b=\gamma=c=1$, $\alpha=2.00120$, and $\nu=0.5$; $\Delta x:=x(t)-x_s$, $\Delta y:=y(t)-y_s$. The necessary conditions for the existence of a noise-induced limit cycle $\alpha_{cr}(\nu)<\alpha<\alpha_{cr0}$ are satisfied: $\alpha_{cr}(\nu)=2.00096$ and $\alpha_{cr0}=2.00223$. (b) Time evolution of mean prey density x (upper curve) and predator density y (lower curve) obtained by solving Eqs. (8) and (19) for the limit cycle. The period of oscillations $T\approx 28.05$. Note that the predator-prey cycles exhibit a delay of $\Delta t=4.14$ between prey and predator maxima. The time is dimensionless as scaled by Eq. (7).

Figure 1(b) demonstrates the formation of a stable limit cycle around the unstable equilibrium point $x_s=0.392880$, $y_s=0.219985$, at a moderate value of the switching rate $\nu=0.5$, at which $\alpha_{cr0}>\alpha>\alpha_{cr}(\nu)$. The inner shaded region in the figure corresponds to the orbit starting at $x_0=0.392880$, $y_0=0.220035$. The orbit is spiral and tends to a limit cycle (the shaded area contains about 127 spiral cycles). The shaded domain outside the stable limit cycle corresponds to the orbit, which tends also to the limit cycle (the initial data are: $x_0=0.392890$, $y_0=0.220045$).

As in the case described in Fig. 1(b), the capturing rate α is very close to the critical capturing rate $\alpha_{cr}(\nu)$ [$\alpha=1.696216$, $\alpha_{cr}(0.5)=1.696206$], the amplitudes of the noise-induced oscillations are very small. Thus, the result of Fig. 1(b) is mainly of a theoretical interest, whereas the oscillations of a biological relevance are characterized by not-too-small values of the amplitude. However, it is remarkable that the size of the limit cycle increases rapidly as the capturing rate $\alpha>\alpha_{cr}$ is increased. An obvious yet interesting biological implication of this circumstance is that a variation of the correlation time of environmental fluctuations can cause oscillations of average prey-population and predator-population sizes with relatively large amplitudes, even in the case of small amplitudes a of fluctuations (cf. Fig. 3).

Furthermore, from Eq. (A5) it follows that in the long time regime, $t\to\infty$, the variance of X_i is relatively small, suggesting that all prey-population densities are distributed in a narrow interval around the mean, even in the case of a wider initial distribution. The macroscopical mean-field oscillations with small variance suggest a strong synchronization of "microscopic" degrees of freedom, i.e., synchronization of individual prey-population dynamics, despite the presence of noise.

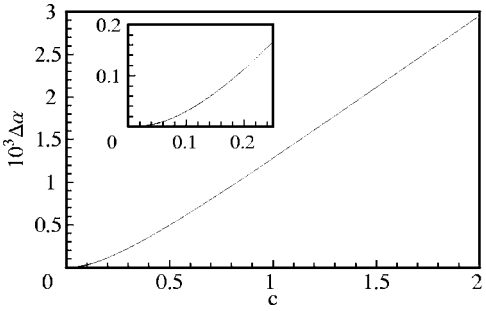

FIG. 4. Typical dependence of $\Delta\alpha=\alpha_{cr0}-\alpha_{cr}(\nu_m)$ on the exponent c [See Eq. (2)] computed from Eqs. (13), (14), and (18), while $\alpha_{cr}(\nu_m)$ is the minimal value of critical capturing rate as ν is varied (cf. Fig. 2). Parameter values $a^2=0.01$, $d=0.5$, $\beta=0.78$, $\omega=0.179487$, and $G(r)=0.56$ are used.

Figure 3 shows a colored-noise-induced stable limit cycle at $a^2=0.01$, $d=0.5$, $\beta=0.78$, $b=\gamma=c=1$, $\alpha=2.0012$, and $\nu=0.5$. It is seen that the amplitudes of population size oscillations are relatively large, 12% for preys and 9% for predators. The period of the oscillations, $T=28.05$, perfectly agrees with the result computed from Eq. (16), 27.97. In addition the phase lag, (the delay between prey and predator maxima), as a fraction of cycle period, is 14.8%, which is smaller than in the case of "classic" predator-prey cycles (the quarter-cycle delay).

As the testing of ecological models based on the generalized Verhulst self-regulation raises the important issue of how different self-regulation mechanisms can influence the behavior of stochastic complex systems, we will shortly consider the dependence of α_{cr} on the exponent c. The quantity of central interest is the difference $\Delta\alpha=\alpha_{cr0}-\alpha_{cr}(\nu_m)$, where $\alpha_{cr}(\nu_m)$ is the minimal value of the critical capturing rate [Eq. (13)]. The typical dependence of $\Delta\alpha$ on the exponent c is displayed in Fig. 4. It can be seen that the interval of the capturing rate $\Delta\alpha$, where noise-induced Hopf bifurcations are possible, increases monotonically as c increases. Hence, models with greater values of c are more sensitive to environmental fluctuations than models with a lower c.

IV. CONCLUDING REMARKS

The effect of colored environmental fluctuations on the dynamics of $(N+1)$-species ratio-dependent predator-preys models, in particular, on the appearance of Hopf bifurcations and related reentrant transitions is addressed in this work. The presence of colored fluctuations of the carrying capacities of prey populations has a profound effect on ecosystems described by Eqs. (3) and (2), rearranging its parameter space so that in a certain region colored noise can induce transitions from an equilibrium state to a state where stable oscillations of populations occur as well as transitions from a stable limit cycle to an equilibrium state, even in the case of

a low noise amplitude. The key factor is noise correlation time. When the control parameter α (prey capturing rate) is located near the bifurcation point between a stable focus and a limit cycle, an increase of noise correlation time can cause oscillations of the mean prey-population and predator-population sizes. Moreover, corresponding transitions are found to be reentrant, i.e., at a higher value of the correlation time the oscillations disappear and the system approaches the equilibrium state. This result that the fluctuations of the carrying capacities of preys can induce Hopf bifurcations and reentrant transitions is somewhat surprising because, in the corresponding deterministic models (noise is absent), the critical prey capturing rate α_{cr} as well as asymptotic behavior of the solutions of the system (8) are independent of the carrying capacity K.

The phenomenon is robust enough to survive modifications of the noise, the predator functional response g, as well as the prey's self-regulation mechanism. For example, the noise can be either a telegraph process with an amplitude a or a Gaussian stationary process. Evidently, Gaussian noise implies the possibility of obtaining negative values of the carrying capacity. Such a case has no biological meaning but, as the Gaussian distribution is narrow enough (the variance a^2 is sufficiently small), the exponentially small negative tail does not affect our results, if restricted to the first order in a^2.

We would like to emphasize that the phenomenon considered in this work is of a qualitatively different nature from recently found effects where nonmonotonous response of nonlinear dynamical systems as a function of noise correlation time has been reported in contexts of coherence resonance [24]. In models considered in Ref. [24], colored fluctuations are added to the deterministic control parameter of bifurcations, but our model fluctuations occur in the carrying capacity K that in the deterministic case is independent of the occurrence of bifurcations. To our knowledge, the noise-correlation-time-induced Hopf bifurcations and corresponding reentrant transitions considered in this work have not previously been discussed in the context of ecological models.

Most of the mean-field results considered in this work are based on the local stability analysis. Hence, many questions concerning the global qualitative behavior of solutions of the model are still open. We note that for deterministic ratio-dependent systems, in general, local stability of the equilibrium state does not imply global asymptotic stability [19]. The numerical calculations based on Eqs. (8) and (19) show that the trivial equilibrium $E_1(0,0)$ has its own basin of attraction in the phase space (x,y), even if there exists a nontrivial stable or unstable equilibrium (with a stable limit cycle) $E_3(x_s,y_s)$. Coexistence of these two different attractors, either with its own basin of attraction, can cause dramatic consequences for the ecosystem [15,25] up to extinction. The answer to the question very important in an ecological context, whether variations of the correlation time of environmental fluctuations can cause extinction of a heterogeneous predator-prey system, is a subject of future investigations. Finally, we believe that the model and results discussed here are also of interest in other fields, such as, e.g., in autonomous chemical reaction systems [26].

ACKNOWLEDGMENTS

This work was partly supported by the Estonian Science Foundation Grant No. 5943 and the International Atomic Energy Agency Grant No. 12062.

APPENDIX: DERIVATION OF THE SELF-CONSISTENCY EQUATIONS (8)

The crucial step in the derivation of the mean-field self-consistency equations (8) is to find the formal solution of the first equation in Eqs. (3) with the scaling (7) and Eqs. (2) and (5). We find that

$$X_i = [\dot{M}(t)]^{1/c}\left[\frac{1}{x_{0i}^c} + c\int_0^t \frac{\dot{M}(t^*)}{[K_i(t^*)]^c}dt^*\right]^{-(1/c)}, \qquad \text{(A1)}$$

where $\dot{M}(t)=(\mathrm{d}/\mathrm{dt})M(t)$, $x_{0i}=X_i(0)$, and

$$M(t) = \int_0^t \exp\left[c\int_0^{t^{**}}\left[1-\frac{\alpha y}{\langle X\rangle}g\left(\frac{\langle X\rangle}{y}\right)\right]dt^*\right]dt^{**}. \qquad \text{(A2)}$$

Here we have used the fact that in mean-field approximation the size average $\bar{x}$ equals the statistical average $\langle X\rangle$. As mentioned in Sec. II, we assume that the dispersion a^2 of noise $aZ_i(t)$ is sufficiently small, $a^2 \ll 1$, and therefore, a perturbation approach can be used. Namely, we expand the right side of Eq. (A1) up to the second order in a small noise amplitude a and, in what follows, confine ourselves to the terms proportional to a^2, i.e., we ignore the higher moments of the noise $aZ_i(t)$. For the sake of simplicity, the distribution of initial data, x_{0i}, is assumed to be symmetric with a small variance σ^2, $\sigma^2 \ll (\langle x_{0i}\rangle)^2$. Taking into account Eqs. (6) and (7) and confining ourselves to the terms proportional to a^2 and σ^2, we get, after averaging Eq. (A1) over the initial distribution and realizations of the noise $aZ_i(t)$, the following integral equation:

$$\langle X(t)\rangle = \left[\frac{\dot{M}}{\kappa + c\gamma M}\right]^{1/c}\left\{1 + \frac{1+c}{2}[\kappa + c\gamma M]^{-2}\right.$$
$$\times\left[\frac{\sigma^2}{x_0^{2(c+1)}} + \frac{2\gamma c\chi}{x_0^{c+1}}\int_0^t \dot{M}(t^*)e^{-\nu t^*}dt^*\right.$$
$$\left.\left. + a^2c^2\gamma^2\int_0^t\int_0^t e^{-\nu|t^*-t^{**}|}\dot{M}(t^*)\dot{M}(t^{**})dt^*dt^{**}\right]\right\}, \qquad \text{(A3)}$$

where

$$\gamma = \frac{1}{K^c}\left(1 + \frac{c(c+1)}{2}a^2\right), \quad \kappa = \frac{1}{x_0^c}\left(1 + \frac{c(c+1)\sigma^2}{2x_0^2}\right),$$

$x_0=\langle x_{0i}\rangle=\langle X(0)\rangle$, and $\chi := \langle aZ_i(t), X_i(t)\rangle_{|t=0}$

Now it is easy to see that the integral equation (A3) is equivalent to the first differential equation in Eqs. (8) with the initial conditions

$$\dot{x}_0 \equiv \langle X(0)\rangle^{\cdot} = x_0\left[1 - \frac{\alpha y_0}{x_0} g\left(\frac{x_0}{y_0}\right) - \gamma x_0^c\left(1 + \frac{c(c+1)(\sigma^2 - 2x_0\chi)}{2x_0^2}\right)\right],$$

$$\ddot{x}_0 \equiv \langle X(0)\rangle^{\cdot\cdot} = \dot{x}_0\left\{(c+1)\frac{\dot{x}_0}{x_0} - c\left[1 - \alpha\frac{y_0}{x_0} g\left(\frac{x_0}{y_0}\right)\right]\right\} + \alpha x_0\left[\frac{\dot{x}_0}{x_0} + d - \beta g\left(\frac{x_0}{y_0}\right)\right]\left[\frac{y_0}{x_0} g\left(\frac{x_0}{y_0}\right) - g'\left(\frac{x_0}{y_0}\right)\right] + c^2(c+1)\gamma^2 x_0^{2c+1}\left[a^2 + \frac{\sigma^2}{x_0^2} - \frac{\chi(\nu + 2c\gamma x_0^c)}{c\gamma x_0^{c+1}}\right], \quad \text{(A4)}$$

where $y_0 \equiv y(0)$ and $g'(\xi) \equiv [d_g(\xi)]/d\xi$.

The result (A3) may be used on Eq. (A1) to derive an expression for the variance of prey-population densities $X_i(t)$. By analogous derivation of Eq. (A3), from Eqs. (A1) and (A3) the formula for the variance $\sigma^2(X)$ can be found

$$\sigma^2(X) = \frac{\langle X\rangle^2}{(\kappa + c\gamma M)^2}\left[\frac{\sigma^2}{x_0^{2(c+1)}} + \frac{2c\gamma\chi}{x_0^{c+1}}\int_0^t \dot{M}(t^*)e^{-\nu t^*}dt^* + a^2c^2\gamma^2\int_0^t\int_0^t e^{-\nu|t^*-t^{**}|}\dot{M}(t^*)\dot{M}(t^{**})dt^*dt^{**}\right]. \quad \text{(A5)}$$

From Eq. (A5), it follows that in the long time regime, $t\to\infty$, the dispersion $\sigma^2(X)$ is independent of the initial distribution of x_{0i}, being of the same order as the noise variance a^2, i.e., $\sigma^2(X) \leqslant a^2\langle X\rangle^2$, if $t\to\infty$.

The corresponding formula for the correlation between noise and prey-population abundances is

$$\langle aZ_i(t)X_i(t)\rangle = \frac{\langle X\rangle e^{-\nu t}}{[\kappa + c\gamma M]}\left[\frac{\chi}{x_0^{c+1}} + c\gamma a^2\int_0^t \dot{M}(t^*)e^{\nu t^*}dt^*\right]. \quad \text{(A6)}$$

From Eq. (A6), it follows that, if $t\to\infty$, $\langle aZ_i, X_i\rangle \leqslant a^2\langle x\rangle$. Finally, we note that the initial values for the first and second time derivatives of X cannot be chosen freely [see Eqs. (A4)], being fully predetermined by the initial values of x, y, variance of preys σ^2, and correlation $\chi \equiv \langle aZ_i(0), X_i(0)\rangle$.

[1] O. V. Ushakov, H.-J. Wünsche, F. Henneberger, I. A. Khovanov, L. Schimansky-Geier, and M. A. Zaks, Phys. Rev. Lett. **95**, 123903 (2005).

[2] R. L. Badzey and P. Mohanty, Nature (London) **437**, 995 (2005); B. McNamara, K. Wiesenfeld, and R. Roy, Phys. Rev. Lett. **60**, 2626 (1988); A. D. Hibbs, A. L. Singsaas, E. W. Jacobs, A. R. Bulzara, J. J. Bekkedahl, and F. Moss, J. Appl. Phys. **77**, 2582 (1995); M. L. Spano, M. Wun-Fogle, and W. L. Ditto, Phys. Rev. A **46**, 5253 (1992); L. Fronzoni, R. Mannella, P. V. E. McClintock, and F. Moss, *ibid.* **36**, 834 (1987); R. Kawai, X. Sailer, L. Schimansky-Geier, and C. Van den Broeck, Phys. Rev. E **69**, 051104 (2004); G. S. Jeon and M. Y. Choi, Phys. Rev. B **66**, 064514 (2002).

[3] H. Haken, Rev. Mod. Phys. **47**, 67 (1975); W. Horsthemke and R. Lefever, *Noise Induced Transitions: Theory and Applications in Physics, Chemistry and Biology* (Springer-Verlag, Berlin, 1984); K. Wiesenfeld and F. Moss, Nature (London) **373**, 33 (1995); L. Gammaitoni, P. Hänggi, P. Jung, and F. Marchesoni, Rev. Mod. Phys. **70**, 223 (1998); J. García-Ojalvo and J. M Sancho, *Noise in Spatially Extended Systems* (Springer-Verlag, Berlin, 1999).

[4] Hu Gang, T. Ditzinger, C. Z. Ning, and H. Haken, Phys. Rev. Lett. **71**, 807 (1993).

[5] A. S. Pikovsky and J. Kurths, Phys. Rev. Lett. **78**, 775 (1997); A. Neiman, P. I. Saparin, and L. Stone, Phys. Rev. E **56**, 270 (1997); B. Lindner, J. García-Ojalvo, A. Neiman, and L. Schimansky-Geier, Phys. Rep. **392**, 321 (2004); C. B. Muratov, E. Vanden-Eijnden, and E. Weinan, Physica D **210**, 227 (2005).

[6] L. I and J.-M. Liu, Phys. Rev. Lett. **74**, 3161 (1995).

[7] I. Z. Kiss, J. L. Hudson, G. J. Escalera Santos, and P. Parmananda, Phys. Rev. E **67**, 035201(R) (2003).

[8] L. Becks, F. M. Hilker, H. Malchov, K. Jürgens, and H. Arndt, Nature (London) **435**, 1226 (2005); J. L. Jost, J. F. Drake, A. G. Frederickson, and H. M. Tsuchiya, J. Bacteriol. **113**, 834 (1973); B. Dennis, R. A. Desharnais, J. M. Cushing, and R. F. Costantino, J. Anim. Ecol. **66**, 704 (1997); G. F. Fussmann, S. P. Ellner, K. W. Shertzer, and N. G. Hairston Jr., Science **290**, 1358 (2000); T. Yoshida, L. E. Jones, S. P. Ellner, G. F. Fussmann, and N. G. Hairston Jr., Nature (London) **424**, 303 (2003); W. A. Nelson, E. McCauley, and F. J. Wrona, Nature (London) **433**, 413 (2005).

[9] P. Turchin, *Complex Population Dynamics: A Theoretical/Empirical Synthesis* (Princeton University Press, Princeton, 2003).

[10] *Population Cycles: The Case for Tropic Interactions*, edited by A. A. Berryman (Oxford University Press, London 2002).

[11] J. M. G. Vilar and R. V. Solé, Phys. Rev. Lett. **80**, 4099 (1998); G. Abramson and D. H. Zanette, Phys. Rev. E **57**, 4572 (1998); B. Houchmandzadeh, *ibid.* **66**, 052902 (2002); B. Drossel and A. McKane, J. Theor. Biol. **204**, 467 (2000); P. Chesson, Theor Popul. Biol. **64**, 345 (2003); N. Kinezaki, K. Kawazaki, F. Takasu, and N. Shigesada, Theor Popul. Biol. **64**, 291 (2003); V. Kaitala and E. Ranta, Proc. R. Soc. London, Ser. B **268**, 1769 (2001); A. McKane, D. Alonso, and R. V. Solé, Phys. Rev. E **62**, 8466 (2000); A. Caruso, M. E. Gargano, D. Valenti, A. Fiasconaro, and B. Spagnolo, Fluct. Noise Lett. **5**, L349 (2005); B. Spagnolo, A. Fiasconaro, and D. Valenti, *ibid.* **3**, L117 (2003).

[12] R. Mankin, A. Ainsaar, A. Haljas, and E. Reiter, Phys. Rev. E **65**, 051108 (2002); R. Mankin, A. Sauga, A. Ainsaar, A. Haljas, and K. Paunel, *ibid.* **69**, 061106 (2004); A. Sauga and R. Mankin, *ibid.* **71**, 062103 (2005).

[13] O. L. Petchey, A. Gonzalez, and H. B. Wilson, Proc. R. Soc.

London, Ser. B **264**, 1841 (1997); J. Ripa and P. Lundberg, *ibid.* **263**, 1751 (1996); H. Caswell and J. E. Cohan, J. Theor. Biol. **176**, 301 (1995); F. V. De Blasio, Phys. Rev. E **58**, 6877 (1998); M. Heino and M. Sabadell, Biol. Conserv. **110**, 315 (2003).

[14] A. A. Berryman, Ecology **73**, 1530 (1992).

[15] C. Jost, O. Arino, and R. Arditi, Bull. Math. Biol. **61**, 19 (1999).

[16] R. M. May, Science **177**, 900 (1972); R. M. May, *Stabiliy and Complexity in Model Ecosystems* (Princeton University Press, Princeton, 2001).

[17] R. Arditi and L. R. Ginzburg, J. Theor. Biol. **139**, 311 (1989).

[18] R. Arditi and A. A. Berryman, TREE **6**, 32 (1991); R. Arditi, L. R. Ginzburg, and H. R. Akcakaya, Am. Nat. **138**, 1287 (1991); R. Arditi, N. Perrin, and H. Saiah, Oikos **60**, 69 (1991); I. Hanski, TREE **6**, 141 (1991); H. R. Akcakaya, R. Arditi, and L. R. Ginzburg, Ecology **76**, 995 (1995); C. Cosner, D. L. DeAngelis, J. S. Ault, and D. B. Olson, Theor Popul. Biol. **56**, 65 (1999).

[19] Y. Kuang and E. Beretta, J. Math. Biol. **36**, 389 (1998); S.-B. Hsu, T.-W. Hwang, and Y. Kuang, *ibid.* **42**, 489 (2001).

[20] M. Bandyopadhyay and J. Chattopadhyay, Nonlinearity **18**, 913 (2005).

[21] *Advanced Ecological Theory*, edited by J. M. McGlade (Blackwell Science, London, 1999); J. D. Murray, *Mathematical Biology* (Springer-Verlag, Berlin, 1993).

[22] Y. A. Kuznetsov, *Elements of Applied Bifurcation Theory* (Springer-Verlag, New-York, 1998).

[23] V. I. Klyatskin, *Stohasticheskie Uravneniya i Volny v Sluchaino-Neodnorodnyh Sredah* (Nauka, Moskva, 1980) (in Russian).

[24] J. L. Cabrera and F. J. de la Rubia, Europhys. Lett. **39**, 123 (1997); J. M. Buldú, J. García-Ojalvo, C. R. Mirasso, M. C. Torrent, and J. M. Sancho, Phys. Rev. E **64**, 051109 (2001); J. L. Cabrera, J. Gorroñogoitia, and F. J. de la Rubia, *ibid.* **66**, 022101 (2002); S. Brugioni, D.-U. Hwang, R. Meucci, and S. Boccaletti, *ibid.* **71**, 062101 (2005).

[25] M. Scheffer, S. Carpenter, J. A. Foley, C. Folke, and B. Walker, Nature (London) **413**, 591 (2001); S. Rinaldi and M. Scheffer, Ecosystems **3**, 507 (2000); J. Vandermeer and P. Yodzis, Ecology **80**, 1817 (1999).

[26] Z. Hou and H. Xin, Phys. Rev. E **60**, 6329 (1999).